the case with absorption spectroscopy. In many cases, even the convoluted spectra of the radial breathing mode region in roped samples can be fit reliably without considering the second derivative as the component peaks can be seen as distinct peak shoulders. However, the complexity of the RBM region increases considerably with higher density of material. Hence, any analysis of thick nanotube networks requires a reasonably robust fitting routine that can pick out RBM components not directly visible in the spectrum itself. We suggest one analysis route that uses the increased resolution afforded by higher order derivatives to deconvolute complicated RBM spectra where spectral features like peak shoulders are too subtle. The following sections detail the procedure of a deconvolution routine that provides stable and interactive analysis of RBM spectra. Variations of this routine could be used to fit large spectral sets by simply eliminating the interactive component or by modifying it slightly.

5.3.1 Introduction to second derivatives

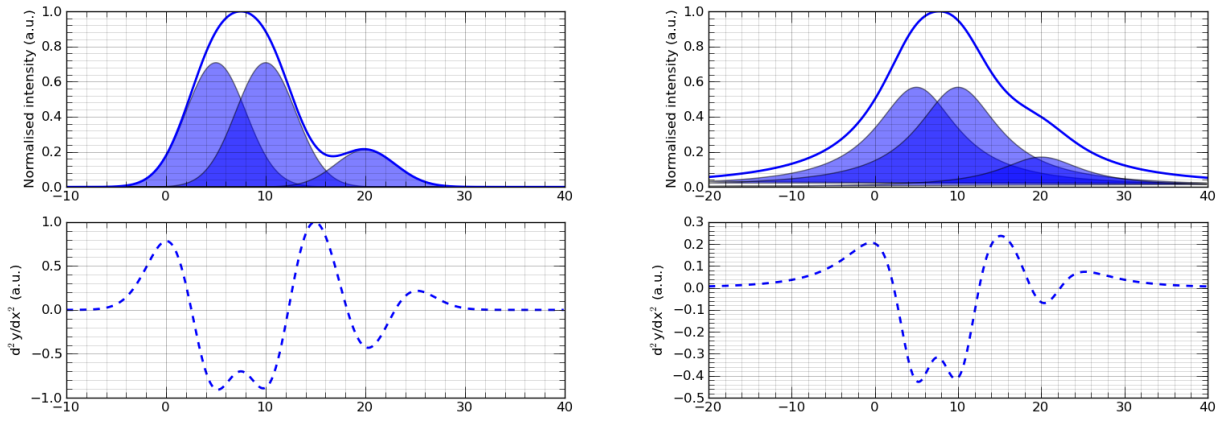

(a) Gaussian (b) Lorentzian

Figure 5.7: Convoluted spectra comprised of component gaussians (a) and lorentzians (b) with FWHM (Γ) = 6.

Empirically, it can be shown that the second derivative can resolve two peaks provided their peak maxima are separated by at least 80% of the FWHM. At this limit, the composite spectrum looks like a single peak (top plots in Figure 5.7) while the second derivative clearly resolves two peaks. The second derivatives (bottom plots of Figure 5.7) of the gaussian and lorentzian were calculated analytically using the formulae given in Eq. 5.3 and Eq. 5.4 respectively. The constants a, b and c are the intensity, position and width respectively. For the gaussian, c is proportional to the linewidth by the relation: $c = \Gamma/(2\sqrt{(2\log 2)})$ while c is the half-linewidth for a lorentzian.

In their highly-detailed article, Mark and Workman [101] highlight several important parameters to be aware of when calculating higher order derivatives. They make a particular note

of the wavelength resolution for the numerical evaluation of second derivatives. They illustrate that increasing the wavelength spacing leads to errors in the shape of calculated derivatives while increasing the derivative intensity. This trade-off, while interesting, does not impact the numerical calculation of second derivatives from Raman spectra due to the high wavelength resolution available using fine gratings (e.g. 1800 lines/mm). Raman spectra collected for this chapter have a resolution of 0.01 nm compared to the 1 nnm resolution typical of absorption spectra. We have compared the second derivative spectra from the raw data compared with interpolated data and noticed little to no difference between the two indicating that the raw data is good enough for all analyses of the second derivative.

$$d^2y/dx^2 = (-a/c^2)\exp\left[-\left(\frac{(x-b)}{\sqrt{2}c}\right)^2\right] + \left[(-a/c^2)(x-b)^2\right]\exp\left[-\left(\frac{(x-b)}{\sqrt{2}c}\right)^2\right] \tag{5.3}$$

$$d^2y/dx^2 = (2a/c^2)\left(\frac{((2x-2b)^2(1/(c^2)) - (1+((x-b)/c)^2)}{(1+((x-b)/c)^2)^3}\right) \tag{5.4}$$

5.3.2 Fitting spectra

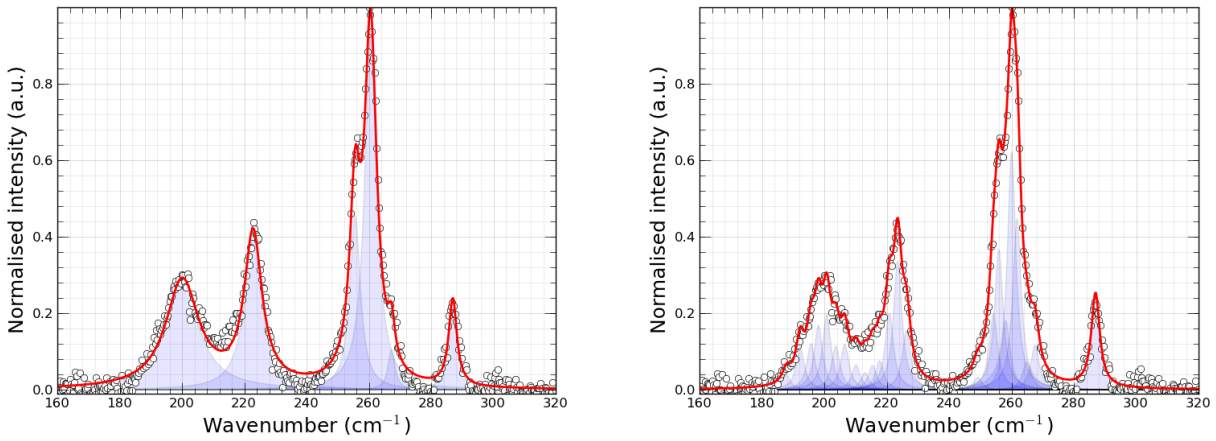

(a) Software peak detection

(b) Manual peak fitting

Figure 5.8: Deconvolution of a RBM spectrum of a thin film using a typical GUI software with lorentzians.

A typical fitting routine begins with a manual inspection of the spectrum using visual clues like peak shoulders and bumps to indicate components. A graphical user interface is often used to select the position of the component peaks. Once the user is satisfied that all the component peaks are included, constraints are applied on each peak and the minimisation algorithm is run. Minimisation routines that utilise the Levenberg-Marquadt algorithm are particularly sensitive to initialisation parameters and it is up to the user to ensure that all initial values are not too far away from the optimal value. Nonetheless, fitting spectra with three free parameters

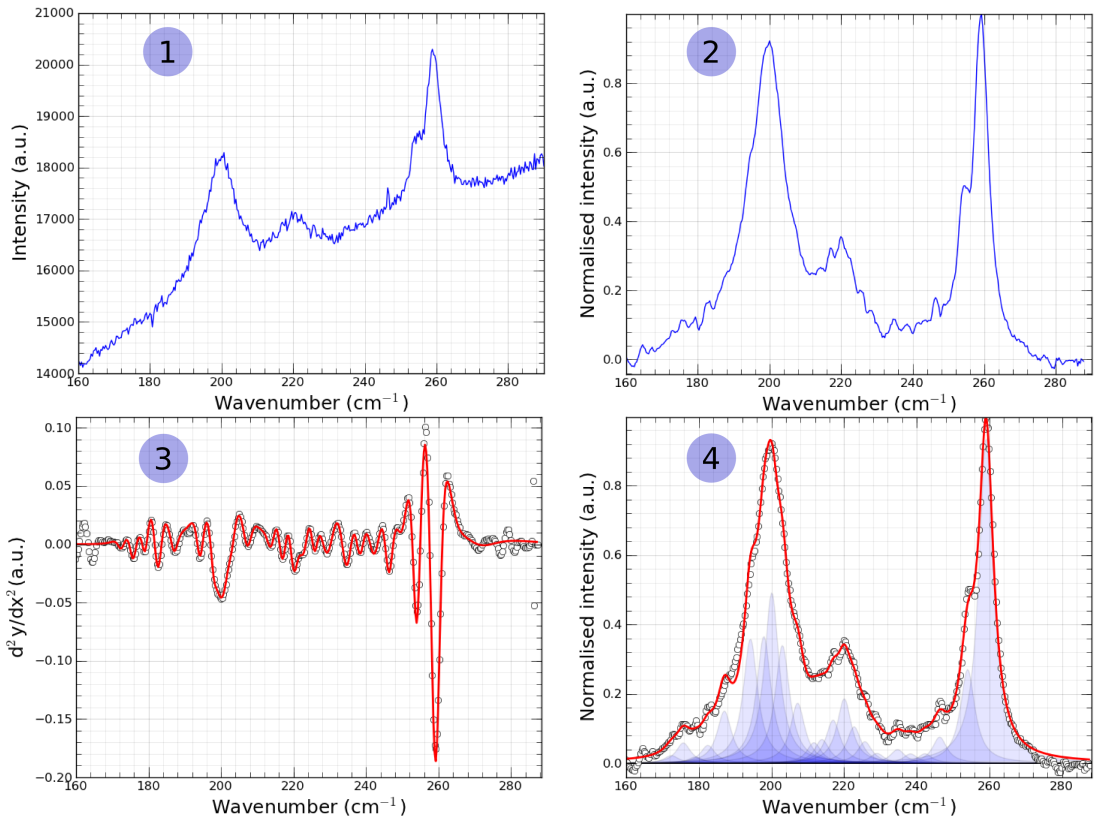

Figure 5.9: Flowchart showing the analysis procedure from raw data to the final fit.

peak becomes progressively less stable and accurate as the number of components increase. When confronted with a spectrum with very few clear shoulders (Figure 5.8), both user and software run into the same trouble highlighted above. Each peak now no longer corresponds to a single nanotube of some chirality (n, m) and there is little physical significance in such a fit.

In order to track the parameters of individual RBMs such as the linewidth, position or intensity, across different samples, we chose to fit the RBM spectra with a slightly more complex procedure than the typical one described in the above paragraph. The flowchart in Figure 5.9 shows that the analysis follows a series of steps from treating the data to the final fit.

1. Raw spectrum

2. Spectrum smoothed using a Savitzky-Golay filter with a window of 15 points and order 3. A linear background is subtracted from the raw data.

3. The second derivative is calculated from the smoothed data in 2. after an additional smoothing using a standard triangular-window moving average. This extra smoothing step ensures that extraneous noise features are not picked up by the second derivative. The second derivative is then fit with a user-specified combination of peaks. The plot shown here has been fit to 12 component gaussians. The fit is engineered such that the second calculated second derivative fit to the calculated second derivative of the 12 components.

4. The peak positions fitted in the above step and a single linewidth for all peaks are used to constrain the fit to the spectrum. The fitted spectrum is further analysed for negative (unphysical) intensities. In the case of negative intensities (which usually occur for very small features), the peak is removed from the list and then the spectrum refitted. This step is both a check of the fit quality and stability. In the case of a fit with negative intensity components, the second fitting round rejects these peaks and refits with the remaining peaks. When the fit contains no negative peaks, this second minimisation checks the stability of the original fit.

The benefit of the fitting procedure described here is the quantity of information that is suddenly available for further analysis compared to the traditional single step fitting. As per the original intentions, the RBM spectra of heavily roped SWNTs can be deconvoluted into component peaks that largely correspond to individual tubes. Unambiguous assignments with unique (n, m) are not likely for all the deconvoluted peaks in the case of our chosen laser line but could be achieved with lines that excite a smaller population of tubes (e.g. 514.5 nm).

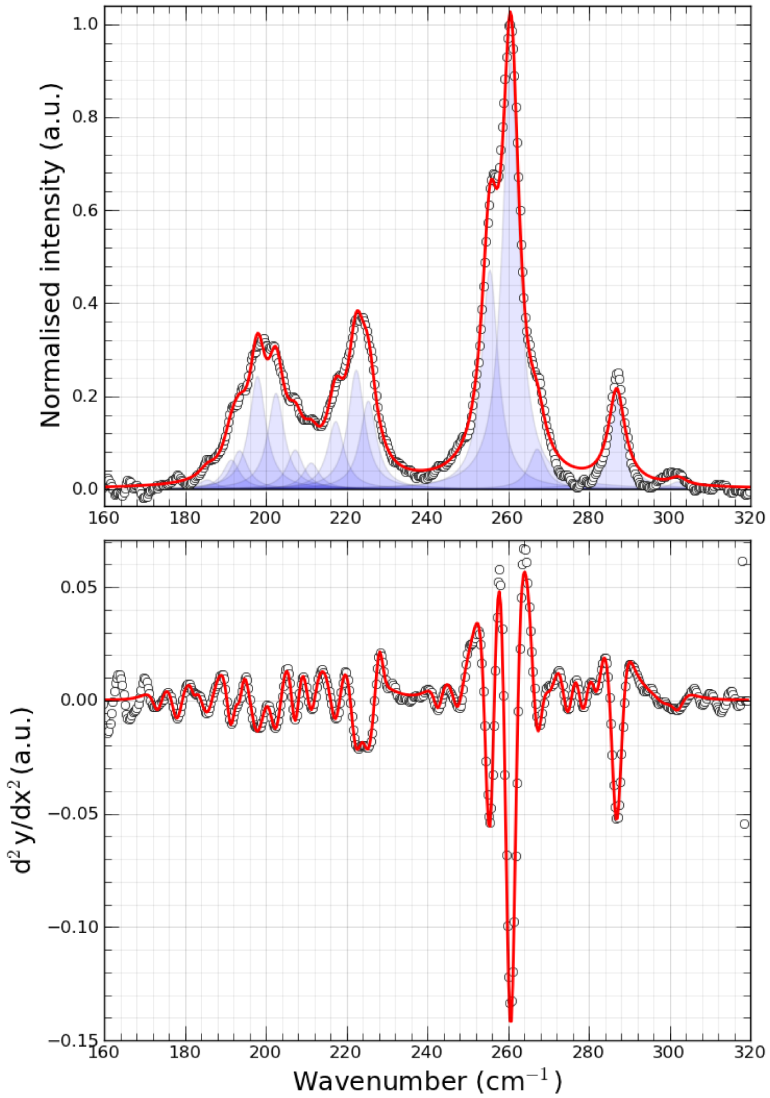

Figure 5.10: Comparing deconvoluted spectra with the second derivative.